Valence-band photoemission from GaAs(100)-$c(4\times4)$

T. Strasser, C. Solterbeck, and W. Schattke
Institut für Theoretische Physik und Astrophysik, Christian-Albrechts-Universität, Leibnizstrasse 15, D-24098 Kiel, Germany

I. Bartoš, M. Cukr, and P. Jiříček
Institute of Physics, Academy of Sciences of the Czech Republic, Prague, Czech Republic

(Received 17 July 2000; published 1 February 2001)

The energy distributions of photoelectrons emitted from the $c(4\times4)$ reconstructed GaAs(100) surface are carefully analyzed within the one-step model of photoemission, thus demonstrating that such calculations work for large unit cells. It is used for detailed interpretation of published and new angular resolved He I experimental data. Surface-related features are found and their localization and symmetry are determined. Backfolding of the electron energy bands and its splitting at the reduced Brillouin zone's boundaries lead to smaller energy dispersion of electron surface states and resonances. The experimentally observed longer period of a surface resonance than that corresponding to the translation symmetry of the reconstructed surface is confirmed and explained. The existence of two surface states near the upper valence-band edge is verified. One major difference between the theory and the experiment is found that cannot be explained by means of the one-step model for a perfectly reconstructed surface.

DOI: 10.1103/PhysRevB.63.085309 PACS number(s): 79.60.Bm, 73.20.At, 71.20.Nr

I. INTRODUCTION

As a function of growth conditions, several reconstructions of the polar surface GaAs(100) have been detected during molecular-beam-epitaxy (MBE) growth. The $c(4\times4)$ reconstruction, which is obtained after cooling the sample to room temperature, represents a stable structure, the geometry of which has been studied recently.[1,2] Besides scanning tunneling microscopy, also a comparison between theoretical and experimental reflectance anisotropy data allows us to identify correlations between structural properties and optical features.[3] *Ab initio* calculations reveal in detail binding and diffusion properties of adatoms and of arsenic dimer dynamics during growth.[4,5] Less attention has been devoted to the electronic structure of GaAs(100)-$c(4\times4)$,[6–8] and the interpretation of experimental angular-resolved photoemission spectra was based on the direct-transition model of photoemission.[9]

The analysis of GaAs(100)-$c(4\times4)$ from normal-emission data[7] concluded that all major sharp peaks observed result from direct transitions from valence bands of the bulk. Investigations, using also off-normal spectra,[8,9] revealed two surface bands below the top of the valence bands. The $k_\parallel$ dispersion, extracted from the topmost peak, does not correspond to the translational symmetry of the reconstructed surface, however. In particular, along $\bar{\Gamma}\bar{J}$, the topmost surface state shows only the simple (1×1) periodicity, whereas the periodicity is doubled along $\bar{\Gamma}\overline{J'}$.[9] The surface-related features will be investigated in detail and clarified here.

Geometrical rearrangements of atoms in the topmost layers are reflected in the changes of the diffraction patterns of reflection high-energy electron diffraction (RHEED) and of low-energy electron diffraction (LEED). Reconstructed surfaces can be expected to have their characteristic surface electronic structure. Indeed, such changes have been reported in surface-sensitive electron spectroscopies, such as photoelectron spectroscopy,[6,7] where in energy distribution curves (EDCs) for 2×4, $c(4\times4)$, and 4×6 reconstructions substantial differences in the upper part of the valence band have been observed. Also, our calculations performed for the ideal surface and the $c(4\times4)$ reconstruction predict the induced changes to be non-negligible.[10] The possible temptation to ascribe the changed parts in the experimental EDCs from different surfaces to surface states can be misleading. The fact that only the topmost atomic layers are changed does not imply that bulk features in the spectra are preserved: the emitted electron, though originating from the bulk of the crystal, undergoes specific scattering in topmost atomic layers also. The possibility of the theoretical description providing contributions from individual atomic layers gives a rather unique means to determine the bulk or surface origin of the EDC feature under consideration. This, together with even finer tracing of the origin within the layer (atom, orbital), will be used for the interpretation of the GaAs(100)-$c(4\times4)$ spectra here.

Photoelectron spectroscopy is known to be a surface-sensitive technique, and the three-step model assumptions about the decomposition of the whole process into independent parts are not exact and lead to remarkable inaccuracies. For excited electrons localized at the surface, all three parts take place in the same region and the electron interference effects have to be respected. This leads to the one-step model of photoemission. The deviations from the conservation of the momentum perpendicular to the surface can be expected to be relatively small for the processes with bulk electrons; they are absent for true surface states (with zero dispersion in the direction perpendicular to the surface) but could be profound for surface resonances with mixed character of bulk and surface states. Especially in more accurate investigations, the EDCs calculated in the one-step model have to be compared with experimental data similarly to the analysis of LEED intensity profiles for the full surface crystallography determination.

 ©2001 The American Physical Society

This paper is organized as follows. After a short introduction in experimental and theoretical basics, the electronic structure of the GaAs(100)-$c(4\times4)$ surface is discussed. Afterwards, the measured and calculated photoemission spectra in off-normal emission, associated with the $\bar{\Gamma}\,\bar{J}$ direction, are presented. The origin of different experimental peaks is explained and differences and commonness are discussed.

II. EXPERIMENT

The GaAs layer growth was performed in the Kryovak/DCA Instruments MBE apparatus using an As tetramer under RHEED control. A special sample holder, consisting of two parts locked together, was used for the growth. Its one part fits the MBE facility transport system while the other is adjusted to the photoelectron spectrometer. Substrate temperature was kept at 580 °C during the growth, with a beam equivalent pressure relation of As to Ga around 10. (2×4) surface reconstruction was maintained during growth and RHEED specular beam oscillations were monitored: good quality of the layer-by-layer growth as well as that of the final surface has been observed. After deposition of about 100 nm of GaAs, temperatures of both the substrate and the As cell were gradually lowered to show the $c(4\times4)$ reconstruction, which remained preserved until room temperature was reached.

The grown GaAs samples were immediately transported under vacuum into the photoelectron spectrometer ADES 400 (VG Scientific). For this purpose, a portable ultrahigh-vacuum transport chamber has been constructed.[11] During the transfer, when the chamber was evacuated by the ion pump, the transport chamber pressure was 10^{-9} mbar. Special care was devoted to cleaning the dead space between the transport and spectrometer chambers after joining them together. A diffusion pump of the differential pumping system of the photoelectron spectrometer combined with heating to 150 °C was used. After reaching 10^{-9} mbar, the sample was transferred to the spectrometer manipulator. The total time needed for the sample transfer from MBE to ADES was about 2 h.

The surface reconstruction and sample orientation after the transfer have been checked by LEED. Surface purity control performed by x-ray photoemission spectroscopy showed no impurities. For electron excitation, He I radiation from the discharge lamp (VG Scientific) has been used. The energy analyzer, set to the constant energy mode of 5 eV, worked with an energy resolution of 150 meV and an angular resolution $\pm1.3°$.

III. SYMMETRY AND CALCULATION

In As-rich surfaces of GaAs(100), the arsenic atoms have a tendency to form dimers. It is generally accepted that dimer vacancies are responsible for various enlarged periodicities of ordered reconstructed surfaces. For the $c(4\times4)$ structure, a model with blocks of three adsorbate As dimers has been proposed on the basis of scanning tunneling microscopy investigations.[12] Quantitatively, full surface geometry has been obtained recently by the energy-minimization

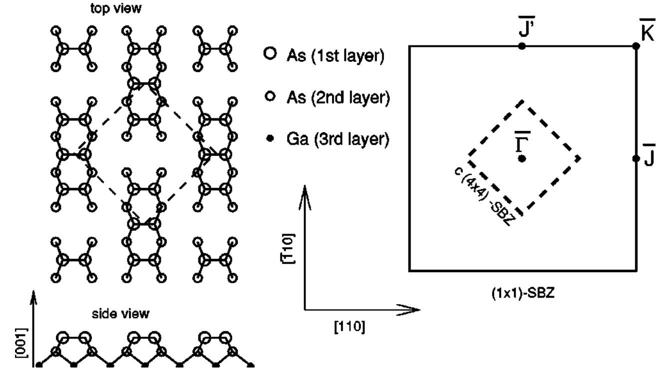

FIG. 1. Model of the $c(4\times4)$ reconstructed GaAs(100) surface with reconstructed unit cell dashed (left) and surface Brillouin zones for the ideal (outer square) and the reconstructed (inner square) surface (right).

procedure.[13] We are adopting these data in the one-step photoemission calculation: the reconstruction is fully included in the initial states, whereas the final states are taken for the ideal 1×1 surface. The square Brillouin zones corresponding to the ideal (1×1) and reconstructed $c(4\times4)$ surfaces are shown in Fig. 1, where also some higher symmetry points are given for the ideal surface. The angular-resolved EDC spectra have been measured and calculated in the [110] direction along the axis of surface dimers (the polar angle θ is measured from the surface normal). Measurement fixes the surface parallel direction via the RHEED pattern of the intermediate (2×4) reconstruction. The Brillouin-zone corner of the $c(4\times4)$ structure in this direction is situated in the middle between $\bar{\Gamma}$ and $\bar{J}$. The $\bar{J}$ from the edge of the ideal structure Brillouin zone thus becomes $\bar{\Gamma}$ after reconstruction. Backfolding of the electron band structure into the smaller Brillouin zone reduces the $E(k)$ period in the k space to one-half.

This shorter k periodicity of $E(k)$ for the reconstructed surface should also be reflected in $k_{\parallel}$-resolved surface densities of states (SDOS) with correspondingly shorter repetition in θ according to the relation between the polar angle and the surface component of the electron wave vector:

$$k_{\parallel}=\frac{\sqrt{2mE_{\mathrm{kin}}}}{\hbar}\sin\theta,$$

where E_{kin} is the kinetic energy of the emitted photoelectron.

Electrons from the center of the surface Brillouin zone $\bar{\Gamma}$ are responsible for normal photoemission. For GaAs(100) and an excitation energy of 21.2 eV (with 5.25 eV for the work function, as in Ref. 14), the polar angle $\theta=22°$ is connected with electrons from the vicinity of the ideal Brillouin-zone boundary $\bar{J}$. Thus, at polar angles around 22° off-normal, the SDOS peak positions for the reconstructed surface have to be nearly the same as in normal emission. This contrasts with the ideal surface, where no repetition is achieved in this range of polar angles.

The increased translational period along the surface of reconstructed surfaces, accompanied by the reduction of the Brillouin-zone dimensions [and the corresponding backfold-

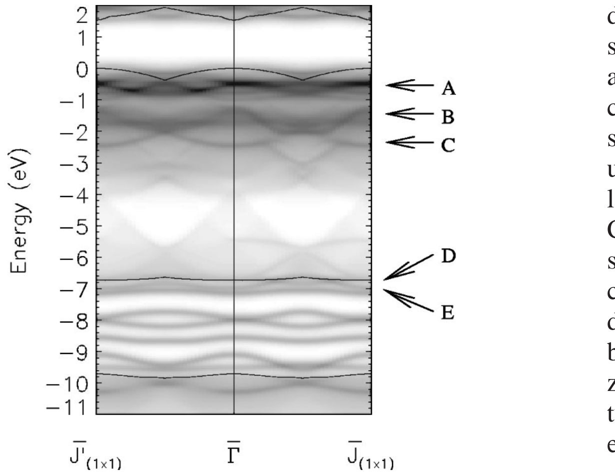

FIG. 2. Surface band structure of GaAs(100)-$c(4\times4)$ (gray shaded, high density is dark) and the projected bulk band structure (boundaries marked by solid lines) for two perpendicular segments from $\bar{\Gamma}$ to the Brillouin zone corner (0 eV corresponds to the VBM); letters denote the surface-state position at $\bar{\Gamma}$ according to Fig. 3.

ing of branches of the electron energy dispersion $E(k)$, Fig. 2], have to result in an increased number of $E(k)$ branches reflected in angular-resolved photoemission by denser-spaced EDC peaks with decreased dispersion.

The photocurrent is calculated within the one-step model. For details, see Refs. 14 and 15. In this ''golden rule'' type formulation of the photoemission process, the photocurrent I at the photon energy $h\nu$ is given by

$$I \sim \sum_{i,j} \langle \Phi^{*}_{\mathrm{LEED}}(E_{\mathrm{fin}},k_{\parallel}) | \mathbf{A_0}\cdot\mathbf{p} | \Psi_i \rangle G_{i,j}(E_{\mathrm{fin}}-h\nu,k_{\parallel}) \times \langle \Psi_j | \mathbf{p}\cdot\mathbf{A_0} | \Phi^{*}_{\mathrm{LEED}}(E_{fin},k_{\parallel}) \rangle .$$

The vector potential of the incident light $\mathbf{A}_0$ is kept constant, $\mathbf{p}$ denotes the momentum operator, and $k_{\parallel}$ is the parallel momentum. The initial states are represented by a half-space Green's function. This Green's function $G_{i,j}$ is given in a layer-resolved linear combination of atomic orbitals Ψ_i. Our basis set consists of the 4s and 4p atomic orbitals of gallium and arsenic. The associated Hamilton matrix is calculated according to the extended Hückel theory. In this theory, a small number of parameters is used to determine the Hamilton matrix from the matrix of orbital overlaps. The parameters for GaAs are specified by fitting the bulk band structure and are listed in Ref. 16. These parameters can be used for any change of the atomic distances at the surface, because the distance dependence is given by the respective overlap. The electronic structure of the surface is determined by the calculation of the $k_{\parallel}$-resolved density of states (DOS) from the half-space Green's matrix $G_{i,j}$, the same as used for the photocurrent. The Green's matrix takes into account relaxation and reconstruction at the surface. The hole-lifetime broadening in the Green's function is fixed to 200 meV.

The final state of photoemission is a time-reversed LEED state Φ^{*}_{LEED} with final-state energy E_{fin}. Its wave function is determined by matching the solution of the complex band structure to the vacuum solution, representing the surface by a step potential. The position of the step is determined by comparing calculated photoemission spectra for different step positions with experimental ones. One step position is used for all spectra. The solution within the bulk is calculated by the empirical pseudopotential method, developed by Cohen and Bergstresser.[17] In some special case, the final states were calculated with full inclusion of the surface reconstruction, employing *ab initio* pseudopotentials.[18,19] The damping of the wave function inside the crystal is described by the imaginary part of an optical potential. The parametrization of the optical potential is given in Ref. 14. Its magnitude monotonically increases from 0.42 eV for 11 eV to 1.71 eV for 24 eV final-state energy.

Here, final states of the unreconstructed surface are used. Incorporation of the reconstruction would be rather demanding with regard to computational time for the whole series of spectra needed here. Therefore, only a single test (see Fig. 5) has been performed to justify our simplified approach. Also, our previous experience with other reconstructed and relaxed surfaces (Refs. 10 and 20) supports the approximate treatment of final states used here.

IV. RESULTS AND DISCUSSION

The surface electronic structure can be gained from $k_{\parallel}$-resolved SDOS and it is shown for two higher-symmetry lines in Fig. 2. Numerous branches of surface states and resonances with little dispersion are found. Close to the valence-band top, a surface-state band (A), almost dispersionless, is seen at -0.6 eV. From symmetry-resolved decomposition for the four topmost atomic layers (see Fig. 3), the p_z character of the As dimer can be seen and thus this surface-state band represents dangling bonds on dimers directed into the vacuum. The deeper-lying band (B), situated at -1.6 eV, is formed by p_x, p_y orbitals of the arsenic dimers (bridge bonds) and by p_z orbitals from the underlying plane of As atoms (Fig. 3). A weaker resonance (C) at around -2.5 eV has mostly p_z character of As situated just below the dimers. A few more rather flat surface bands are located between -6.5 and -9 eV. The states (D) and (E) are related to the s orbitals from the arsenic dimers. The former one (D) is located near the upper edge of the heteropolar gap. Surface and bulk densities of states corresponding to the band structure of Fig. 2 are shown in Fig. 4. They are calculated with respect to $k_{\parallel}$ and can be directly compared with the photoemission spectra, presented below. It shows that the state (A) has only weak resonance in the bulk, while the surface resonance (B) is located in a region where considerable contributions from the bulk are expected.

The EDCs shown in Fig. 5 are taken along the (110) azimuth for the He I excitation ($h\nu=21.2$ eV): polar angles θ are measured from the surface normal with negative values counted towards the direction of photon beam ($\theta=56°$). The calculated EDCs (thick lines) are compared with experimental counterparts (thin lines).

A rather pronounced experimental peak is situated around -6 eV over the whole range of polar angles. This peak was

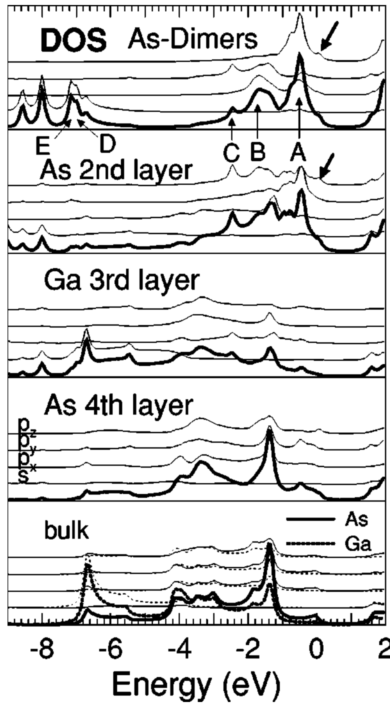

FIG. 3. Density of electron states at $\bar{\Gamma}$ for GaAs(100)-$c(4\times4)$ resolved according to orbital contributions (thin lines) from four topmost atomic layers, thick lines for total DOS. Furthermore, the DOS for the bulk atomic layers is shown. All panels have the same scale; hole lifetime amounts to 200 meV.

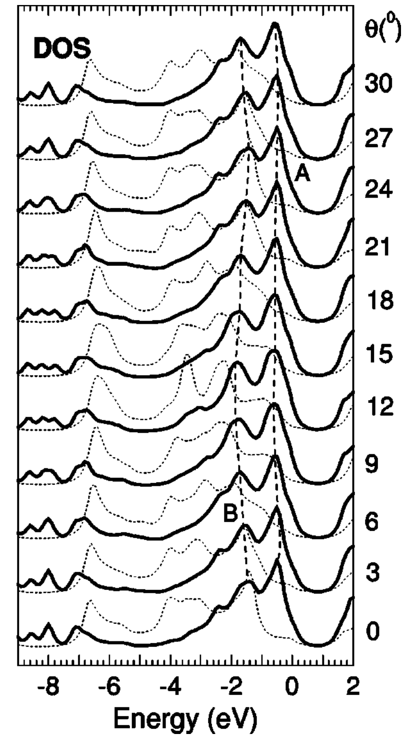

FIG. 4. $k_{\parallel}$-resolved electron densities of states for surface (first four atomic layers, solid lines) and for the bulk (dotted lines) GaAs(100)-$c(4\times4)$ along $\bar{\Gamma}\,\bar{J}$. An angle of 22° corresponds to $\bar{J}$ at a binding energy of 0 eV in photoemission with $h\nu=21.2$ eV.

also detected for the whole range of excitation energies in photoemission investigations performed with synchrotron radiation,[7,9] but its intensity was much smaller than in this experiment. In normal photoemission, it is generally associated with the bulk critical point X_3 of the one-dimensional density of states.[7] The increased density of states below -6 eV is clearly manifested also here in the bulk DOS (Fig. 4), but the corresponding feature in the calculated EDC is missing. In theoretical spectra, there is a small peak (g) at an energy above -6.8 eV (clearly visible at off-normal angles approaching $\pm30°$). A closer analysis shows that this emission is caused by As s orbitals, which are localized in the first two surface layers and are related to the surface resonance (D) (see Fig. 2) and not to the band edge. The strongly dispersing structure (c') moving from around -6 eV to higher energies when decreasing the polar angle θ has its counterpart in a weak structure in the experimental data (in particular, between $\theta=21°$ and $30°$). Like the dispersive structure (f), it results from direct transitions. Only the strong experimental peak at -6 eV has no counterpart in theoretical curves. No significant influence from light polarization and angle of incidence on this result was observed in the calculations. As in our calculation, the full band structure of the electron final states is taken into account, and no related feature is found in the theoretical EDC spectra (this result did not change even if full surface reconstruction were considered in the final states). Another mechanism should be responsible for its presence in the experimental spectra (provided, e.g., by surface disorder). We attribute the failure of the theoretical structure (f) to yield the correct experimental intensity also to the surface disorder. Peak (f) is clearly a bulk feature, see Fig. 6 for $\theta=30°$, and might be hidden by surface contamination, which influences both initial and final states.

Apart from these discrepancies, the main experimental peaks and their θ dependence are in fair agreement with theoretical calculations. The pronounced peaks (d) at -8 eV in theoretical spectra for polar angles between $-12°$ and $+12°$ result from the simplified treatment of final electron states here (ideal 1×1 surface); these structures are suppressed when the true $c(4\times4)$ reconstruction is taken into account also for final states.[21] As an example, Fig. 5 presents a spectrum in normal emission (dotted line, right-hand side), which is calculated with the true reconstruction considered in the final state.

Published experimental band-mapping data pointed out that the periodicity of the surface state near the upper valence-band edge is not the same in photoemission as estimated from LEED or RHEED.[8,9,22] While the surface state shows the doubled periodicity along $\bar{\Gamma}\,\bar{J}'$ as expected for the $c(4\times4)$ geometry, it shows the simple periodicity of the (1×1) surface along $\bar{\Gamma}\,\bar{J}$. However, in experiment the monotonic dispersion along $\bar{\Gamma}\,\bar{J}$ is found in the energy range between 0.68 eV and 1.0 eV, which is wider than in the surface band structure of Fig. 2.

The fact that the topmost peak in the EDC (a) (just below the valence band top $E=0$, Fig. 5) displays larger dispersion than expected from the SDOS (Fig. 4) is due to the influence of an intervening bulk contribution at low polar angles. This

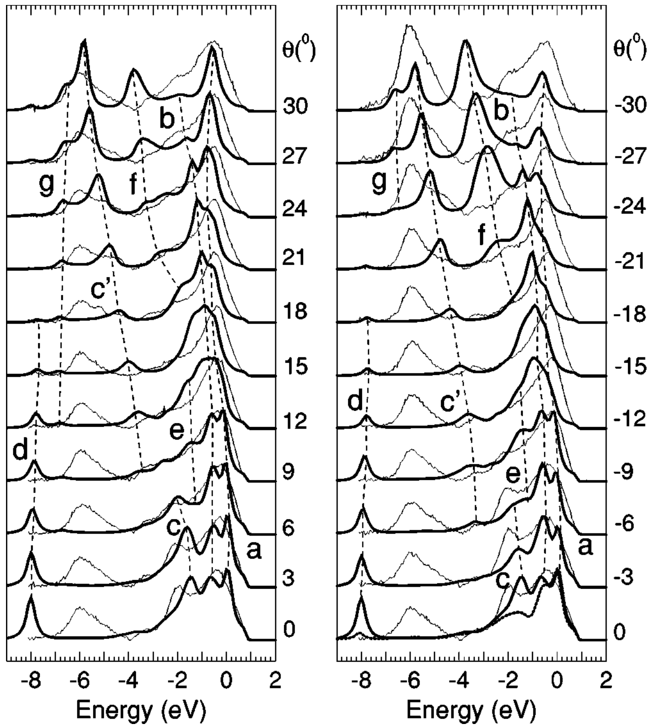

FIG. 5. Angular-resolved photoemission spectra for GaAs(100)-$c(4\times4)$ (experiment, thin lines; theory, thick lines) excited by He I radiation incident at 56° polar angle for a set of emission polar angles θ, i.e., left, moving away from the incident radiation beam (positive θ); right, approaching the incident radiation beam (negative θ). On the right side, also a spectrum in normal emission (dotted line) is presented, which is calculated with the full $c(4\times4)$ reconstruction taken into account in the final states.

is illustrated by the layer-resolved photocurrent.

The layer-resolved contributions to the photocurrent are shown in Fig. 6 for normal emission of electrons and for two off-normal angles in the $\bar{\Gamma}\bar{J}$ direction (in this case, experimental broadening is not applied to make the effects sharper and more visible). Delocalized bulk electron states are responsible for the gradual layer-by-layer increase of the intensities, whereas localized surface states give rise to fully developed structures in the photocurrent within the first layer. Surface resonances, in which a localized character is mixed with the admixture of bulk states, exhibit less regular tendencies. For normal emission, the peak (a) at 0 eV binding energy is clearly related to emission from the surface. It results from a small shoulder in the density of states of the arsenic p_z orbitals, which is marked by arrows in Fig. 3. This interpretation is in accordance with the arsenic p_z matrix elements (not shown), which are the most important in this angle and energy region. The structures (b) and (c) have a clear bulklike character. The latter finding is also confirmed by inspecting the corresponding band structures of initial and final electron states (band mapping, not shown here). It seems that the bulk emission (b) overlaps the emissions from the surface state (A) from Fig. 2, which should be expected by the huge peak in the density of states near -0.6 eV. Increasing the emission angle, the bulk state (b) disperses to higher binding energies and now the emissions from the surface state (A) become visible at -0.6 eV, as expected from surface band structure. Figure 6 shows a clear surface emission for the polar angle of 30°, corresponding to structure (a). So, the interference with bulk emissions introduces an additional dispersion to the surface-state emission, which solves the problem of missing periodicity in experiment mentioned above. This dispersion could not be expected examining only the surface band structure or the density of states.

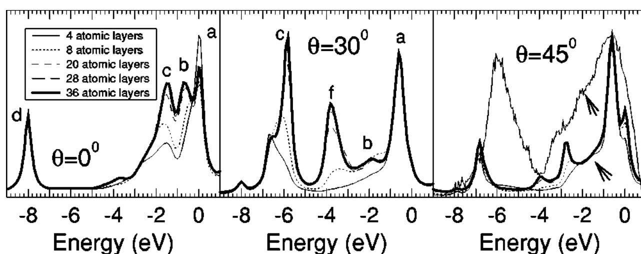

FIG. 6. Layer-resolved contributions, number counted from top, to photoemission intensity for electron emissions: (a) $\theta=0°$, (b) $\theta=30°$, (c) $\theta=45°$. For (c) also experimental data are shown.

The relative ratio of intensities of surface-related peaks to the bulk-related ones when increasing the polar angle is also apparent from Fig. 6, and this confirms the intuitive expectation that the surface sensitivity of the photoemission becomes enhanced when the emission angle of electrons is increased from the surface normal. This can be used for the identification of the surface state (B) (see Fig. 2). Emission from this state can be seen as weak structures (e) in Fig. 5. For these small angles, there are also emissions from bulk states, which have to be taken into account for this structure. At $\theta=45°$, this situation changes. Now the shoulder marked by an arrow in Fig. 6 is clearly related to the surface state (B) and can be identified in the experimental spectra.

Deviations in peak magnitudes between theory and experiment (such as the bulk peak at -4 eV for $\theta=30°$) might be removed if a more detailed description of the imaginary component of the optical potential were considered.[23] Here, the electron attenuation is treated as energy-dependent but homogeneous within the crystal. But other effects not taken into account, such as final states corresponding to the reconstructed surface, could also reduce the differences as observed for the -8 eV theoretical structure.

V. CONCLUSIONS

First one-step calculations for a large unit cell are presented. Experimental photoemission spectra of GaAs(100)-$c(4\times4)$ are compared in detail with theoretical ones.

The major difference between theory and experiment, the entirely dispersionless experimental band at about -6 eV, still remains to be explained. Numerous surface-related features have been found in the EDCs for GaAs(100)-$c(4\times4)$ at energies below the top of the valence band and their orbital symmetry has been determined from corresponding theoretical decomposition. Weakly dispersing surface states and resonances found here confirm general expectations resulting from the reduced dimensions of the Brillouin zones

of reconstructed surfaces and of the corresponding electron band folding of the electron energy bands. Theoretical decomposition of EDCs into contributions from individual atomic layers below the surface enables a clear distinction between bulk- and surface-related features. Differences in the periodicity of a surface state and the expectation from surface reconstruction are explained by an interference between bulk and surface contributions in the photoemission process.

Realistic one-step calculations of photoemission intensities provide a useful basis for the interpretation of experimental energy distribution curves for reconstructed GaAs surfaces.

ACKNOWLEDGMENTS

The work was supported by the BMBF under Contract No. 05 SB8 FKA7 and No. TSR-075-97 and by the project KONTAKT ME090 and the program INFRA2 (Grant No. LB98202).

[1] A.R. Avery, D.M. Holmes, J. Sudijono, T.S. Jones, and B.A. Joyce, Surf. Sci. **323**, 91 (1995).
[2] Q.K. Xue, T. Hashizume, and T. Sakurai, Prog. Surf. Sci. **56**, 1 (1997).
[3] A.I. Shkrebtii, N. Esser, W. Richter, W.G. Schmidt, F. Bechstedt, B.O. Fimland, A. Kley, and R. Del Sole, Phys. Rev. Lett. **81**, 721 (1998).
[4] J.G. LePage, M. Alouani, D.L. Dorsey, J.W. Wilkins, and P.E. Blöchl, Phys. Rev. B **58**, 1499 (1998).
[5] C.G. Morgan, P. Kratzer, and M. Scheffler, Phys. Rev. Lett. **82**, 4886 (1999).
[6] P.K. Larsen, J.H. Neave, and B.A. Joyce, J. Phys. C **14**, 167 (1981).
[7] T.C. Chiang, R. Ludeke, M. Aono, G. Landgren, F.J. Himpsel, and D.E. Eastman, Phys. Rev. B **27**, 4770 (1983).
[8] P.K. Larsen, J.H. Neave, J.F. van der Veen, P.J. Dobson, and B.A. Joyce, Phys. Rev. B **27**, 4966 (1983).
[9] J. Olde, G. Mante, H.P. Barnscheidt, L. Kipp, J.C. Kuhr, R. Manzke, M. Skibowski, J. Henk, and W. Schattke, Phys. Rev. B **41**, 9958 (1990).
[10] T. Strasser, F. Starrost, C. Solterbeck, and W. Schattke, Phys. Rev. B **56**, 13 326 (1997).
[11] P. Jiřı́ček, M. Cukr, V. Kolařı́ik, and S. Koc, Rev. Sci. Instrum. **69**, 2804 (1998).
[12] D.K. Biegelsen, R.D. Bringans, J.E. Northrup, and L.E. Schwartz, Phys. Rev. B **41**, 5701 (1990).
[13] A. Kley, Ph.D. thesis, University of Berlin, 1997.
[14] J. Henk, W. Schattke, H. Carstensen, R. Manzke, and M. Skibowski, Phys. Rev. B **47**, 2251 (1993).
[15] J. Henk, W. Schattke, H.P. Barnscheidt, C. Janowitz, R. Manzke, and M. Skibowski, Phys. Rev. B **39**, 13 286 (1989).
[16] F. Starrost, S. Bornholdt, C. Solterbeck, and W. Schattke, Phys. Rev. B **53**, 12 549 (1996); **54**, 17 226 (1996).
[17] M.L. Cohen and T.K. Bergstresser, Phys. Rev. **141**, 749B (1966).
[18] A. Bödicker and W. Schattke, Phys. Rev. B **55**, 5045 (1997).
[19] C. Solterbeck, O. Tiedje, F. Starrost, and W. Schattke, J. Electron Spectrosc. Relat. Phenom. **88-91**, 563 (1998).
[20] W. Schattke, Prog. Surf. Sci. **54**, 211 (1997).
[21] A. Kistner, Diploma thesis, University Kiel, 1999; available at http://www.tp.cau.de/theo-physik/schattke.
[22] R.D. Bringans and R.Z. Bachrach, in *Proceedings of the 17th International Conference on the Physics of Semiconductors, San Francisco, 1984*, edited by W.A. Harrison (Freeman, San Francisco, 1984).
[23] C. Solterbeck, O. Tiedje, T. Strasser, S. Brodersen, A. Bödicker, W. Schattke, and I. Bartoš, J. Electron Spectrosc. Relat. Phenom. **101-103**, 473 (1999).